RSC Advances

PAPER

View Article Online
View Journal | View Issue

Cite this: *RSC Adv.*, 2025, **15**, 36895

Synthesis, *in silico* and *in vitro* studies of aminopyrimidine hybrids as EGFR TK inhibitors and anti-proliferative agents

Wael Shehta, [a] Basant Farag, [a] Shaker Youssif, *[a] Samar El-Kalyoubi [b] and Sherin M. Elfeky [c]

In this article, two series of pyrimidine hybrids, 2-((4-amino-6-(1,3-dioxoisoindolin-2-yl)pyrimidin-2-yl) thio)-*N*′-(alkylbenzylidene)acetohydrazides (**6a–g**) (Series I) and 6-amino-5-((alkylamino)(phenyl)methyl) pyrimidine-2,4(1*H*,3*H*)-diones (**10a–d**) (Series II), were synthesized using catalyst-free condensation of acid hydrazide **4** with different aromatic aldehydes and nucleophilic substitution reactions of chloromethylpyrimidine with different aliphatic amines , respectively. Compared to gefitinib (IC_{50} = 4.1 ± 0.01 μM) and thalidomide (IC_{50} = 13.4 ± 0.5 μM), compounds **6c** and **10b** exhibited moderate anti-proliferative activity against the MCF-7 breast cancer cell line, with IC_{50} values of 37.7 ± 3.6 and 31.8 ± 2.0 μM, respectively. They demonstrated selective cytotoxicity toward MCF-7 cells over normal WI38 fibroblasts, with IC_{50} values of 87.3 ± 2.6 μM (**6c**) and >100 μM (**10b**). Both compounds showed potent *in vitro* EGFR-TK enzyme inhibition, with IC_{50} values of 0.9 ± 0.03 μM (**6c**) and 0.7 ± 0.02 μM (**10b**). Molecular docking simulations revealed that **6c** and **10b** effectively bind to the EGFR ATP-binding site, forming hydrogen bonds with the key hinge region amino acid Met793, similar to gefitinib. *In silico* studies confirmed that both compounds fit the criteria for orally bioavailable drug candidates, showing high gastrointestinal absorption and no predicted adverse effects on the central nervous system or liver. Additionally, both compounds were predicted to be non-carcinogenic and non-mutagenic.

Received 11th April 2025
Accepted 21st July 2025

DOI: 10.1039/d5ra02524a

rsc.li/rsc-advances

1. Introduction

Cancer remains a leading cause of morbidity and mortality worldwide. Despite considerable advancements in targeted therapies and early detection, many cancers continue to present treatment challenges, particularly due to resistance development and off-target toxicities.[1] One such promising molecular target for designing anti-tumor agents is epidermal growth factor receptor tyrosine kinase (EGFR-TK). EGFR is one of the receptor tyrosine kinases (RTKs).[2] TKs share similar basic structures, including an extracellular ligand binding, a transmembrane, a cytoplasmic tyrosine kinase and a signaling domain. Ligand binding induces dimerization and activation of the tyrosine kinase domain. This consequently leads to autophosphorylation, which enhances cell proliferation and inhibits apoptosis. Moreover, the overexpression of EGFR results in angiogenesis and metastasis, which promote various tumor types, including lung cancer and breast cancer.[3–5] There are three types of EGFR inhibitors: type I, type II and type III. Gefitinib, a type I reversible EGFR inhibitor, is FDA-approved for treating non-small cell lung cancer and breast cancer. This drug inhibits EGFR by interacting with the ATP-binding site, whereby the N1 of its quinazoline ring forms a hydrogen bond with the key amino acid Met793 in the hinge region. It also forms a number of hydrophobic interactions with Leu718, Val726, Lys745, Met766, Leu788, Thr790, and Leu844. Despite its effectiveness, gefitinib has side effects such as skin rash, diarrhea, and loss of appetite, driving the search for more selective EGFR inhibitors with reduced toxicity.[6] Structurally, EGFR TK inhibitors are diverse, including pyrazolines,[7,8] pyrazoles,[9,10] quinazolines,[11–13] coumarins,[14–16] benzothiazoles,[17,18] thiazoles,[19,20] and imidazoles.[21] Different aminopyrimidines were reported to be potent EGFR-TK inhibitors, as shown in Fig. 1. Pyrazolopyrimidine **I** (ref. 22) and dihydropyridopyrimidine **II** (ref. 23) have shown selectivity for EGFR over other tyrosine kinases. These compounds have shown inhibition in the nanomolar range and potential anti-tumor activity against A549 cancer cells. Pyrimidopyrimidines **III** (ref. 24) have been reported to show selective cytotoxicity and the inhibition of EGFR-TK in the nanomolar range. Elmetwally *et al.*[25] reported that compounds IV were capable of inhibiting EGFR-TK in the micromolar range and showed anti-proliferative activity against HCT116, HepG-2 and MCF-7 cell

[a]*Chemistry Department, Faculty of Science, Zagazig University, Zagazig 44519, Egypt. E-mail: syoussif@hotmail.com; syoussif@zu.edu.eg*

[b]*Pharmaceutical Organic Chemistry, Faculty of Pharmacy, Port Said University, Port Said, 42511, Egypt*

[c]*Pharmaceutical Organic Chemistry, Faculty of Pharmacy, Mansoura University, Mansoura 35516, Egypt*

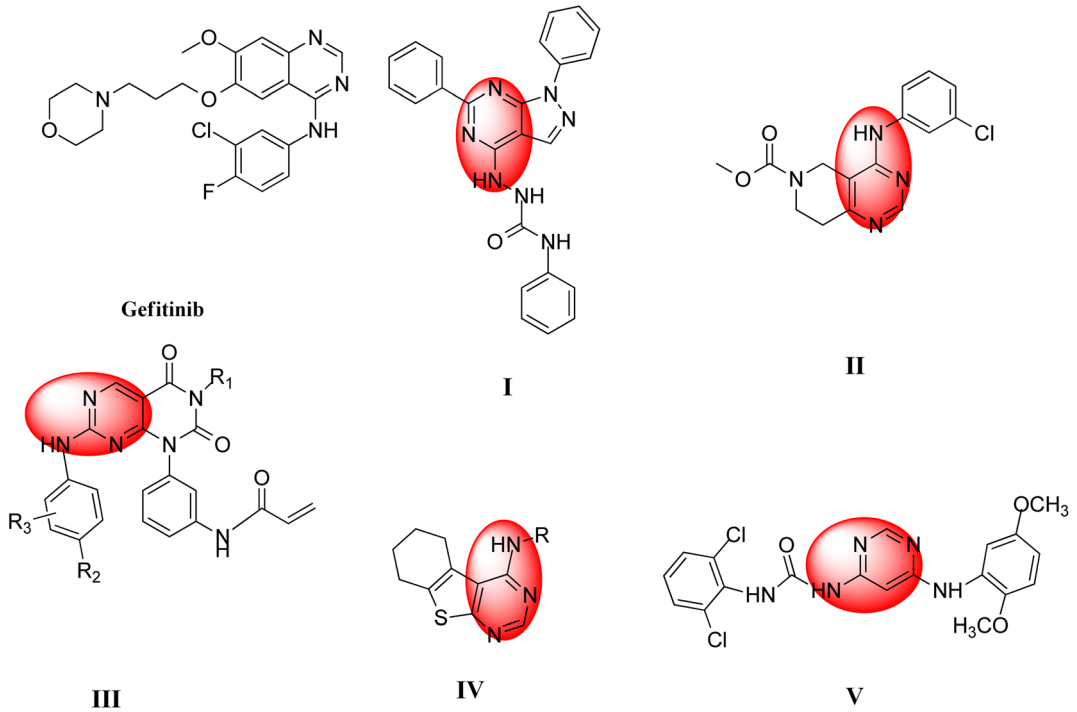

Fig. 1 Different EGFR-TK inhibitors.

lines. These compounds halted the cell cycle at the G2/M phase and induced apoptosis. Molecular docking showed that 4,6-pyrimidinediamine derivatives engaged in hydrogen bonding with Met793 at the ATP binding site of EGFR-TK. Xie *et al.*[26] reported that **V** showed promising anti-proliferative activity through the inhibition of EGFR-TK, and it was capable of reducing the size of the tumor in an *in vivo* study. Aminopyrimidines, as EGFR inhibitors, were reported to share common structural features, including the presence of hydrogen bond acceptor–donor groups that interacted with Met793 and other amino acids. All had bulky aromatic groups through different linkers to allow the hydrophobic interaction in the hydrophobic region of the enzyme. Thalidomide (for structure, see Fig. 2) inhibits angiogenesis and has been

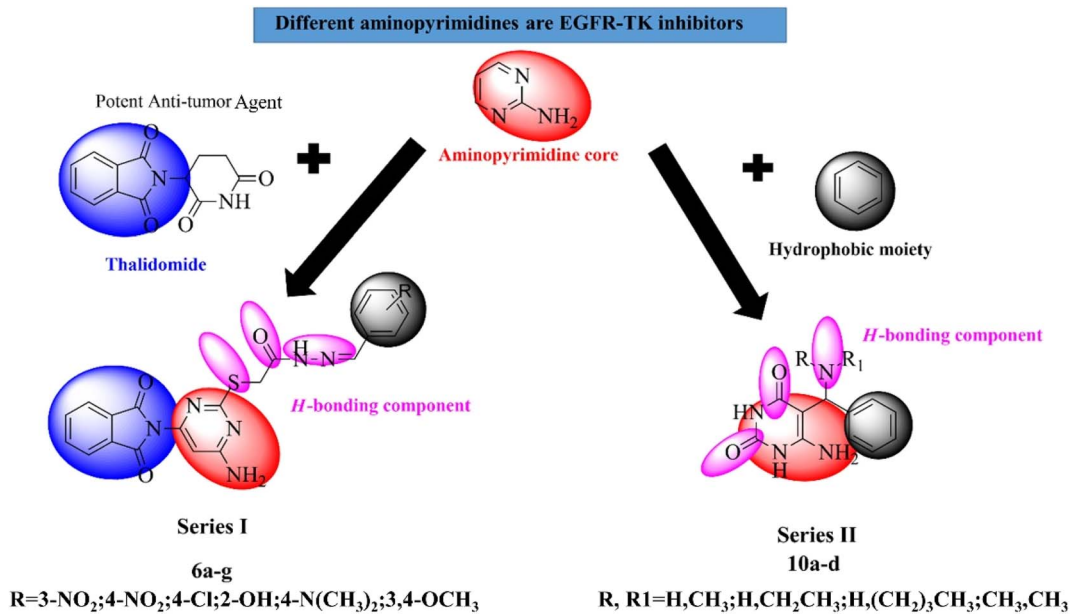

Fig. 2 Design of aminopyrimidine hybrids.

clinically repurposed as an effective anti-tumor agent. Thalidomide, though initially associated with severe teratogenic effects, has been repurposed for its anti-angiogenic and immunomodulatory properties in treating conditions like multiple myeloma and breast cancer.[27] In this paper, we describe the incorporation of the phthalimide moiety of thalidomide as a structural motif in compounds of Series **I**.

1.1. Rationale and design strategy

In the present investigation, pyrimidine was used as the core for designing two series of compounds as potential EGFR-TK inhibitors and anti-proliferative agents. In Series **I**, the phthalimide moiety of thalidomide was hybridized with aminopyrimidines to produce 2-((4-amino-6-(1,3-dioxoisoindolin-2-yl) pyrimidin-2-yl)thio)-*N*′-(alkylbenzylidene)-acetohydrazide (**6a–g**), with two oxo groups of phthalimide introduced at position 6 and the amino group at position 4 of pyrimidine to contribute to the hydrogen bonding, while different substituted phenyl groups were introduced through the hydrazide methyl thio linker at position 2 to contribute to the hydrophobic interaction at the ATP binding site of EGFR-TK. In Series **II** 6-amino-5-((alkylamino)(-phenyl)methyl)pyrimidine-2,4(1*H*,3*H*)-dione (**10a–d**), the phenyl group was introduced at position 5 of 6-aminopyrimidine-2,4-dione through the alkyl aminomethyl linker to participate in hydrogen bonding. Two oxo groups at positions 2 and 4 and an amino group at position 6 were introduced to participate in hydrogen bonding at the EGFR-TK binding site. Fig. 2 shows the design of aminopyrimidine hybrids. The designed compounds were screened for their selective cytotoxicity against MCF-7 and WI-38 compared to gefitinib and thalidomide. Compounds were also screened for the *in vitro* inhibition of the EGFR-TK enzyme compared to gefitinib. Molecular docking simulations were used to study the binding mode of the synthesized compounds at the binding site of the EGFR-TK enzyme. These novel compounds aimed to achieve selective EGFR inhibition and potent anti-proliferative activity with minimal side effects.

2. Materials and methods

2.1. Chemistry

Aldrich Chemical Co., Inc. (WI, USA) provided all the chemicals and reagents used. All the synthesized compounds were detected by TLC with pre-coated plastic sheets of silica gel, and UV (254 nm) was used to visualize the spots. IR spectra were recorded on a Fourier transform infrared 200 spectrophotometer (cm^{-1}) at Zagazig University. The Pye-Uniearn and Beckman spectrophotometers (NY, USA) were utilized for this purpose. A Bruker NMR spectrometer was used to record ^{1}H-NMR and ^{13}C-NMR spectra in DMSO-d_6 at 400 MHz (^{1}H-NMR) and 100 MHz (^{13}C-NMR) using tetramethylsilane as an internal standard (Zagazig University, Zagazig, Egypt). Mass spectra were recorded in the direct inlet section of the mass analyzer (ionization technique: electron impact) using a Thermo Scientific GC-MS model ISQ at the Regional Centre for Mycology and Biotechnology (RCMB), Al-Azhar University, Nasr City, Cairo. For the elemental analysis, a PerkinElmer CHN 2400 was used. Molecular docking simulations were performed in the Computational Chemistry and Molecular Modelling Lab, Pharmaceutical Organic Chemistry Department, Faculty of Pharmacy, Mansoura University, using "Molecular Operating Environment (MOE) 2024.06".

2.1.1 2-(6-Amino-2-mercaptopyrimidin-4-yl)isoindoline-1,3-dione (2). Compound **1** (0.01 mol) and sodium sulfide (0.01 mol) in dry ethanol (50 mL) were heated under reflux with stirring for 15 min. After cooling to room temperature, the resulting precipitate was filtered, washed with cold water, dried and recrystallized from ethanol to give the title compound as a white solid (93%): m.p. = 266–268 °C; ^{1}H-NMR: 4.22 (s, 1*H*, $CH_{Pyrimidine}$), 7.29 (s, 2*H*, NH_2), 7.48–7.52 (t, J = 8.8 Hz, 2*H*, Ar–$H_{Phthalimide}$), 8.16–8.18 (d, J = 8.8 Hz, 2*H*, Ar–$H_{Phthalimide}$), 12.60 (s, 1*H*, SH); ^{13}C-NMR: 81.77, 130.34, 132.54, 134.96, 163.01, 168.11, 170.10, 176.38; IR ν_{max} cm^{-1}: 3348 (br NH_2), 3068 (CH aromatic), 2820 (CH aliphatic), 2413 (SH), 1698 (C=O); MS: *m*/*z* (intensity%): 272.2 (21) [$M^{\bullet+}$], 197 (21), 176.5 (41), 151.83 (31), 108.09 (26), 90.44 (100); anal. calcd for $C_{12}H_8N_4O_2S$ (272.2): C, 52.93; H, 2.96; N, 20.58; found: C, 52.95; H, 2.97; N, 20.68.

2.1.2 Ethyl-2-((4-amino-6-(1,3-dioxoisoindolin-2-yl) pyrimidin-2-yl)thio)acetate (3). A mixture of compound **2** (0.01 mol) and ethyl bromoacetate (0.01 mol) in absolute ethanol (50 mL) containing potassium carbonate (0.01 mol) was refluxed with stirring for 12 h. After cooling to room temperature, the resulting precipitate was filtered, washed with cold water, dried and recrystallized from ethanol to give the title compound as a white solid (81%): m.p. = 228–230 °C; ^{1}H-NMR: 1.03–1.07 (t, J = 7.2 Hz, 3H, $CH_2\underline{CH}_3$), 3.98 (s, 2H, $S\underline{CH}_2$), 4.15–4.21 (q, J = 7.2 Hz, 2H, $\underline{CH}_2CH_3$), 4.88 (s, 1H, $CH_{Pyrimidine}$), 7.49–7.53 (t, J = 7.2 Hz, 2H, Ar–$H_{Phthalimide}$), 7.82 (s, 2H, NH_2), 8.16–8.18 (d, J = 7.2 Hz, 2H, Ar–$H_{Phthalimide}$); ^{13}C-NMR: 14.26, 45.01, 63.04, 79.91, 130.45, 132.62, 135.01, 166.36, 167.72, 168.25, 168.80, 170.44; IR ν_{max} cm^{-1}: 3408 (br NH_2), 3020 (CH aromatic), 2998, 2850 (CH aliphatic), 1749 (C=O $_{ester}$), 1701 (C=O imide); MS: *m*/*z* (intensity%): 358.86 (44) [$M^{\bullet+}$], 313 (19), 285.62 (31), 207.89 (57), 162.7 (53), 117.85 (100); anal. calcd for $C_{16}H_{14}N_4O_4S$ (358): C, 53.62; H, 3.94; N, 15.63; found: C, 53.70; H, 3.99; N, 15.68.

2.1.3 2-((4-Amino-6-(1,3-dioxoisoindolin-2-yl)pyrimidin-2-yl)thio)acetohydrazide (4). Compound **3** (0.01 mol) and hydrazine hydrate (0.01 mol) in absolute ethanol (50 mL) were heated under reflux with stirring for 12 h. After cooling to room temperature, the obtained precipitate was filtered, dried, washed with cold water, and recrystallized from ethanol to give the title compound as a light-yellow solid (75%): m.p. = 247–249 °C; ^{1}H-NMR: 3.43 (s, 2H, $S\underline{CH}_2$), 4.36 (s, 1H, $CH_{Pyrimidine}$), 6.76 (s, 2H, $NH_{2\ hydrazide}$, exchangeable by D_2O), 7.77 (s, 2H, $NH_{2\ Pyrimidine}$, exchangeable by D_2O), 8.02–8.06 (t, J = 8.8 Hz, 2H, Ar–$H_{Phthalimide}$), 8.63–8.65 (d, J = 8.8 Hz, 2H, Ar–$H_{Phthalimide}$), 8.89 (s, 1H, NH, exchangeable by D_2O); ^{13}C-NMR: 59.18, 94.61, 121.16, 128.50, 129.83, 135.10, 142.43, 144.92, 146.52, 151.27, 163.06; IR ν_{max} cm^{-1}: 3332, 3272 (br NH_2 & NH), 3015 (CH aromatic), 2919, 2850 (CH aliphatic), 1682 (CO imide), 1626 (CONH); MS: *m*/*z* (intensity%): 344.37 (29) [$M^{\bullet+}$], 240 (34), 144.78 (36), 117.25 (91), 62 (100); anal. calcd for $C_{14}H_{12}N_6O_3S$ (344.37): C, 48.83; H, 3.51; N, 24.41; found: C, 48.90; H, 3.56; N, 24.47.

2.1.4 General method for the preparation of 2-((4-amino-6-(1,3-dioxoisoindolin-2-yl) pyrimidin-2-yl)thio)-*N*′-(alkylbenzylidene)acetohydrazide (6a–g). Compound **4** (0.001 mol) and aromatic aldehydes **5** (0.001 mol) in ethanol (20 mL) were refluxed with stirring for 8–18 h. After cooling to room temperature, the resulting precipitate was filtered, dried, washed using the appropriate solvent, and recrystallized from ethanol.

*2.1.4.1 2-((4-Amino-6-(1,3-dioxoisoindolin-2-yl)pyrimidin-2-yl) thio)-N′-(3-nitrobenz ylidene)acetohydrazide (**6a**).* Aldehyde: *m*-nitrobenzaldehyde; reflux time: 17 h; washing solvent: acetone, color: pale-yellow; yield: 86%; m.p. = 200–202 °C; ^{1}H-NMR: 4.01 (s, 2H, S$\underline{CH}_2$), 5.32 (s, 1H, $CH_{Pyrimidine}$), 6.96 (s, 2H, NH_2), 7.81–7.85 (t, J = 8 Hz, 1H, Ar–H), 8.32–8.41 (*m*, 2H, Ar–H), 8.72 (s, 1H, Ar–H), 8.92 (s, 4H, Ar–H), 9.13 (s, 1H, CH), 11.74 (s, 1H, NH); ^{13}C-NMR: 43.87, 81.48, 122.68, 125.87, 127.60, 130.70, 133.56, 134.47, 135.26, 137.43, 143.41, 148.25, 160.51, 167.94, 169.33, 172.02, 174.45; IR ν_{max} cm^{-1}: 3396 (br NH_2 & NH), 3085 (CH aromatic), 2920, 2855 (CH aliphatic), 1841 (CO imide), 1687 (CONH), 1627 (C=N), 1574, 1353 (NO_2); MS: *m*/*z* (intensity%): 477.7 (40) [M$^{\bullet+}$], 424.87 (27), 408.23 (14), 287.07 (26), 245.35 (64), 216.93 (97), 179.14 (74), 155.42 (100); anal. calcd for $C_{21}H_{15}N_7O_5S$ (477.45): C, 52.83; H, 3.17; N, 20.54; found: C, 52.85; H, 3.20; N, 20.50.

*2.1.4.2 2-((4-Amino-6-(1,3-dioxoisoindolin-2-yl)pyrimidin-2-yl) thio)-N′-(4-nitrobenz ylidene)acetohydrazide (**6b**).* Aldehyde: *p*-nitrobenzaldehyde; reflux time: 8 h; washed with ice water; color: yellow; yield: 98%; m.p. = 205–207 °C; ^{1}H-NMR: 4.00 (s, 2H, S$\underline{CH}_2$), 5.98 (s, 1H, $CH_{Pyrimidine}$), 7.66–7.68 (d, J = 8.8 Hz, 1H, Ar–H), 7.72–7.76 (t, J = 8.8 Hz, 2H, Ar–$H_{Phthalimide}$), 8.00–8.06 (d, J = 8.8 Hz, 2H, Ar–$H_{Phthalimide}$), 8.07 (s, 2H, NH_2, exchangeable by D_2O), 8.15–8.17 (d, J = 8.8 Hz, 2H, Ar–H), 8.36–8.38 (d, J = 8.8 Hz, 1H, Ar–H), 8.86 (s, 1H, CH), 11.52 (s, 1H, NH, exchangeable by D_2O); ^{13}C-NMR: 38.07, 71.14, 123.98, 125.29, 128.68, 129.59, 131.57, 131.71, 132.56, 134.12, 143.49, 145.61, 160.18, 166.93, 168.41, 169.76, 171.13; IR ν_{max} cm^{-1}: 3411, 3307, 3201 (NH_2 & NH), 3012 (CH aromatic), 2920, 2850 (CH aliphatic), 1702 (C=O imide), 1629 (CONH), 1504, 1343 (NO_2); MS: *m*/*z* (intensity%): 477 (36) [M$^{\bullet+}$], 463.35 (41), 415.10 (100), 385,10 (64), 252.53 (46), 205.01 (76), 114,74 (87); anal. calcd for $C_{21}H_{15}N_7O_5S$ (477.45): C, 52.83; H, 3.17; N, 20.54; found: C, 52.88; H, 3.20; N, 22.25.

*2.1.4.3 2-((4-Amino-6-(1,3-dioxoisoindolin-2-yl)pyrimidin-2-yl) thio)-N′-(4-chlorobenz ylidene)acetohydrazide (**6c**).* Aldehyde: *p*-chlorobenzaldehyde; reflux time: 18 h; washed with methanol; color: buff; yield: 77%; m.p. = 218–220 °C; ^{1}H-NMR: 4.04 (s, 2H, S$\underline{CH}_2$), 5.31 (s, 1H, $CH_{Pyrimidine}$), 6.97 (s, 2H, NH_2), 7.58–7.60 (d, J = 8 Hz, 2H, Ar–H), 7.89–7.91 (d, J = 8 Hz, 2H, Ar–H), 8.06 (s, 4*H*, Ar–$H_{Phthalimide}$), 8.71 (s, 1H, CH), 11.72 (s, 1H, NH); ^{13}C-NMR: 43.55, 80.66, 128.73, 129.09, 130.02, 131.13, 132.60, 136.02, 136.89, 144.16, 160.59, 167.34, 168.77, 169.47, 171.07; IR ν_{max} cm^{-1}: 3350, 3168 (br NH_2 & NH), 3068 (CH aromatic), 2843 (CH aliphatic), 1705 (CON), 1651 (CONH), 1624 (C=N); MS: *m*/*z* (intensity%): 468.09 (33) [M^{2+}], 466.27 (49) [M$^{\bullet+}$], 429.11 (100), 426.79 (82), 392.85 (46), 349.37 (42), 309.44 (38), 151.77 (46); anal. calcd for $C_{21}H_{15}ClN_6O_3S$ (466): C, 54.02; H, 3.24; N, 18.00; found: C, 54.05; H, 3.29; N, 18.10.

*2.1.4.4 2-((4-Amino-6-(1,3-dioxoisoindolin-2-yl)pyrimidin-2-yl) thio)-N′-(2-hydroxybenz ylidene)acetohydrazide (**6d**).* Aldehyde: salicylaldehyde; reflux time: 16.15 h; washed with methanol, color: off-white; yield: 88%; m.p. = 211–212 °C; ^{1}H-NMR: 4.00 (s, 2H, S$\underline{CH}_2$), 5.31 (s, 1H, $CH_{Pyrimidine}$), 6.95–6.99 (t, J = 8 Hz, 1H, Ar–H), 7.38–7.40 (d, J = 8 Hz, 1H, Ar–H), 7.40 (s, 2H, NH_2, exchangeable by D_2O), 7.41–7.43 (d, J = 8 Hz, 1H, Ar–H), 7.68–7.70 (d, J = 8 Hz, 1H, Ar–H), 7.89 (s, 1H, CH), 8.07 (s, 1H, NH, exchangeable by D_2O), 9.00 (s, 4H, Ar–$H_{Phthalimide}$), 11.21 (s, 1H, OH, exchangeable by D_2O); ^{13}C-NMR: 41.97, 71.13, 116.52, 118.19, 119.58, 125.16, 128.67, 130.81, 131.55, 132.55, 133.22, 157.54, 158.64, 162.76, 166.92, 170.05, 174.41; IR ν_{max} cm^{-1}: 3612 (OH), 3432 (br NH_2 & NH), 3008 (CH aromatic), 2850 (CH aliphatic), 1708 (CON), 1660 (CONH), 1614 (C=N); MS: *m*/*z* (intensity%): 448.87 (6) [M$^{\bullet+}$], 423.74 (42), 385.40 (70), 317.09 (72), 249.42 (70), 164.52(65), 152.6 (94), 432 (36), 79.8 (100); anal. calcd for $C_{21}H_{16}N_6O_4S$ (448): C, 56.24; H, 3.60; N, 18.74; found: C, 56.28; H, 3.65; N, 18.74.

*2.1.4.5 2-((4-Amino-6-(1,3-dioxoisoindolin-2-yl)pyrimidin-2-yl) thio)-N′-(4-hydroxybenz ylidene)acetohydrazide (**6e**).* Aldehyde: *p*-hydroxybenzaldehyde; reflux time: 14 h; washed with ice water; color: buff; yield: 96%; m.p. = 200–202 °C; ^{1}H-NMR: 3.98 (s, 2H, S$\underline{CH}_2$), 5.29 (s, 1H, $CH_{Pyrimidine}$), 6.94 (s, 2H, NH_2), 6.94–6.96 (d, J = 8 Hz, 2H, Ar–H), 6.96–6.98 (d, J = 8 Hz, 2H, Ar–H), 7.37–7.41 (t, J = 8 Hz, 2H, Ar–$H_{Phthalimide}$), 7.64–7.66 (d, J = 8 Hz, 2H, Ar–$H_{Phthalimide}$), 8.94 (s, 1H, CH), 10.19 (s, 1H, OH), 11.78 (s, 1H, NH); ^{13}C-NMR: 42.46, 71.71, 116.98, 118.47, 120.20, 129.12, 131.48, 132.07, 133.84, 159.00, 163.42, 167.51, 170.25, 172.84, 174.90; IR ν_{max} cm^{-1}: 3727 (OH), 3204 (br NH_2 & NH), 3044 (CH aromatic), 2852 (CH aliphatic), 1705 (CON), 1615 (C=N); MS: *m*/*z* (intensity%): 448.87 (20) [M$^{\bullet+}$], 415.95 (62), 385.40 (68), 317.09 (64), 249.42 (70), 215.72 (60), 152.61 (94), 79.82 (100); anal. calcd for $C_{21}H_{16}N_6O_4S$ (448): C, 56.24; H, 3.60; N, 18.74; found: C, 56.29; H, 3.63; N, 18.82.

*2.1.4.6 2-((4-Amino-6-(1,3-dioxoisoindolin-2-yl)pyrimidin-2-yl) thio)-N′-((4-dimethyl amino)benzylidene)acetohydrazide (**6f**).* Aldehyde: *p*-dimethylaminobenzaldehyde; reflux time: 16 h; washed with ice water; color: orange; yield: 93%; m.p. = 200–202 °C; ^{1}H-NMR: 3.67 (s, 6H, $2CH_3$), 4.57 (s, 2H, S$\underline{CH}_2$), 5.30 (s, 1H, $CH_{Pyrimidine}$), 6.73–6.75 (d, J = 8 Hz, 2H, Ar–H), 7.63 (s, 2H, NH_2), 7.87–7.89 (d, J = 8 Hz, 2H, Ar–H), 8.07 (s, 4*H*, Ar–$H_{Phthalimide}$), 8.46 (s, 1H, CH), 11.09 (s, 1H, NH); IR ν_{max} cm^{-1}: 3328 (br NH_2 & NH), 3011 (CH aromatic), 2850, 2813 (CH aliphatic), 1713 (CON), 1598 (CONH), 1561 (C=N); MS: *m*/*z* (intensity%): 475.05 (9) [M$^{\bullet+}$], 430.53 (36), 354.51 (52), 326.30 (50), 236.55 (38), 123.28 (54), 94.13 (60), 70.62 (100); anal. calcd for $C_{23}H_{21}N_7O_3S$ (475.52): C, 58.09; H, 4.45; N, 20.62; found: C, 58.10; H, 4.49; N, 20.68.

*2.1.4.7 2-((4-Amino-6-(1,3-dioxoisoindolin-2-yl)pyrimidin-2-yl) thio)-N′-(3,4-dimethoxy-benzylidene)acetohydrazide (**6g**).* Aldehyde: veratraldehyde; reflux time: 10 h; washed with ethanol; color: buff; yield: 76%; m.p. = 220–222 °C; ^{1}H-NMR: 3.07 (s, 3H, O$\underline{CH}_3$), 3.15 (s, 3H, O$\underline{CH}_3$), 3.82 (s, 2H, S$\underline{CH}_2$), 5.47 (s, 1H, $CH_{Pyrimidine}$), 6.19 (s, 2H, NH_2), 7.26–7.28 (d, J = 7.2 Hz, 1H, Ar–H), 7.66–7.68 (d, J = 7.2 Hz, 1H, Ar–H), 7.78 (s, 4H, Ar–

$H_{Phthalimide}$), 8.07 (s, 1H, Ar–H), 8.88 (s, 1H, CH), 11.56 (s, 1H, NH); ^{13}C-NMR: 41.14, 63.17, 71.41, 125.46, 126.66, 127.67, 128.90, 130.54, 131.84, 132.43, 132.73, 135.17, 151.79, 165.93, 167.25, 169.10, 170.28, 173.30; IR ν_{max} cm^{-1}: 3297, 3202 (br NH_2 & NH), 3001 (CH aromatic), 2874, 2853 (CH aliphatic), 1700 (CON), 1622 (CONH), 1595 (C=N); MS: *m*/*z* (intensity%): 492.66 (18) [M$^{\cdot+}$], 488.34 (32), 456.16 (74), 390.29 (46), 282.20 (54), 244.70 (72), 131.44 (54), 103.46 (100); anal. calcd for $C_{23}H_{20}N_6O_5S$ (492.51): C, 56.09; H, 4.09; N, 17.06. Found: C, 57.09; H, 4.10; N, 18.01.

2.1.5 General procedure for the preparation of 6-amino-5-(chloro(aryl)methyl)pyrimidine-2,4(1*H*,3*H*)-dione (8a–c). To 6-aminouracil (**7**) (0.2 g, 1.57 mmol) in hot concentrated HCl (30 mL) was added aromatic aldehyde **5** (1.57 mmol). The mixture was heated at 100 °C for 9 (**8a**), 8 (**8b**) and 10 h (**8c**), respectively. After cooling to room temperature, the resulting precipitate was collected by filtration, washed with cold water (5 mL), dried and recrystallized from methanol.

*2.1.5.1 6-Amino-5-(chloro(phenyl)methyl)pyrimidine-2,4(1H,3H)-dione (**8a**).* Aldehyde: benzaldehyde; reflux time: 9 h; yellow crystal; yield: 95%; m.p. = 218–220 °C; ^{1}H-NMR: 5.45 (s, 1H, CH), 6.97 (s, 2H, NH_2, exchangeable by D_2O), 7.82–7.93 (m, 5H, Ar–H), 11.32 (s, 2H, 2NH, exchangeable by D_2O); ^{13}C-NMR: 43.89, 88.63, 123.02, 132,65, 134.42, 165.60, 169.33; IR ν_{max}-cm^{-1}: 3229, 3120 (br, NH_2 & NH), 3061 (CH aromatic), 2853 (CH aliphatic), 1697 (C=O); MS: *m*/*z* (intensity%): 253.67 (26) [M$^+$ + 2], 251.67 (52) [M$^{\cdot+}$], 235.73 (50), 173.98 (54), 119.27 (52), 118.62 (100), 106.33 (82), 90.53 (54); anal. calcd for $C_{11}H_{10}ClN_3O_2$ (251.67): C, 52.50; H, 4.01; N, 16.70; found: C, 52.60; H, 4.02; N, 16.80.

*2.1.5.2 6-Amino-5-(chloro(2-hydroxyphenyl)methyl)pyrimidine-2,4(1H,3H)-dione (**8b**).* Aldehyde: salicylaldehyde; reflux time: 8 h; orange crystal; yield: 96%; m.p. = 276–280 °C; ^{1}H-NMR: 4.99 (s, 1H, CH), 6.95 (s, 2H, NH_2), 7.49–7.53 (t, J = 8 Hz, 2H, Ar–H), 8.03–8.05 (d, J = 8 Hz, 2H, Ar–H), 10.19 (s, 1H, OH), 11.00 (s, 1H, NH), 11.95 (s, 1H, NH); IR (ν_{max} cm^{-1}): 3685 (OH), 3385, 3185 (br, NH_2 and NH), 3070 (CH aromatic), 2850 (CH aliphatic), 1682 (C=O); anal. calcd for $C_{11}H_{10}ClN_3O_3$ (267.67): C, 49.36; H, 3.77; N, 15.70; found: C, 49.46; H, 3.78; N, 15.80.

*2.1.5.3 6-Amino-5-((chloro(4-dimethylamino)phenyl)methyl) pyrimidine-2,4(1H,3H)-dione (**8c**).* Aldehyde: *p*-dimethylaminobenzaldehyde; reflux time: 10 h; red crystal; yield: 96%; m.p. = 255–257 °C; ^{1}H-NMR: 3.02 (s, 6H, 2CH$_3$), 4.61 (s, 1H, CH), 6.77–6.79 (d, J = 8.4 Hz, 2H, Ar–H), 7.23 (s, 2H, NH_2), 7.66–7.68 (d, J = 8.4 Hz, 2H, Ar–H), 9.65 (s, 1H, NH), 11.00 (s, 1H, NH); IR (ν_{max} cm^{-1}): 3367, 3181 (br, NH_2 and NH), 3040 (CH aromatic), 2917, 2825 (CH aliphatic), 1682 (C=O); MS: *m*/*z* (intensity%): 296.88 (30) [M$^+$ + 2], 294.71 (72) [M$^+$], 269.59 (44), 252.32 (54), 173.98 (46), 118.63 (78), 106.33 (100), 84.5 (34); anal. calcd for $C_{13}H_{15}ClN_4O_2$ (294.74): C, 52.98; H, 5.13; N, 19.01; found: C, 53.00; H, 5.18; N, 19.07.

*2.1.5.4 6-Amino-5-(chloro(aryl)methyl)pyrimidine-2,4(1H,3H)-dione (**10a–d**).* General procedure: 6-aminouracil (**1**) (0.2 g, 1.78 mmol) was dissolved in hot concentrated HCl (30 mL), and the appropriate aliphatic amine **9** (namely, methylamine, ethylamine, butylamine, and dimethylamine) (0.27 g, 1.78 mmol) was added. The mixture was refluxed for 14 h for **10a** and **10b** derivatives. Alternately, **10c** and **10d** were heated in a water bath for 8 and 10 h, respectively. After cooling, the formed precipitate was filtered, washed with methanol, dried, and recrystallized from methanol.

*2.1.5.5 6-Amino-5-((methylamino)(phenyl)methyl)pyrimidine-2,4(1H,3H)-dione (**10a**).* Yellow crystal; yield: 43%; m.p. = 240–242 °C; ^{1}H-NMR: 2.36 (s, 3H, CH_3), 4.41 (s, 1H, CH), 5.80 (s, 1H, NH), 6.27 (s, 2H, NH_2), 7.08–7.10 (d, 1H, Ar–H), 7.18–7.25 (m, 4H, Ar–H), 9.25 (s, 1H, NH), 10.02 (s, 1H, NH); ^{13}C-NMR: 43.89, 88.64, 123.02, 132.65, 134.43, 165.61, 169.34; IR (ν_{max} cm^{-1}): 3330, 3229, 3180 (br NH_2 & NH), 3061 (CH aromatic), 2853 (CH aliphatic), 1697 (C=O); anal. calcd for $C_{12}H_{14}N_4O_2$ (246.11): C, 58.53; H, 5.73; N, 22.75; found: C, 58.51; H, 5.71; N, 22.80.

*2.1.5.6 6-Amino-5-((ethylamino)(phenyl)methyl)pyrimidine-2,4(1H,3H)-dione (**10b**).* Orange crystal; yield: 96%; m.p. = 276–280 °C; ^{1}H-NMR: 1.03–1.07 (t, J = 8 Hz, 3H, CH_3), 2.5–2.54 (q, J = 7.2 Hz, 2H, CH_2), 4.26 (s, 1H, CH), 5.11 (s, 1H, NH), 6.86 (s, 2H, NH_2), 6.89 (s, 1H, Ar–H), 7.14–7.15 (d, 1H, Ar–H), 7.26–7.31 (m, 3H, Ar–H), 11.33 (s, 1H, NH), 11.43 (s, 1H, NH); ^{13}C-NMR: 18.55, 45.77, 54.98, 81.57, 128.02, 128.98, 128.71, 128.92, 129.21, 140.41, 150.02, 167.89, 168.05; IR (ν_{max} cm^{-1}): 3385 & 3185 (NH_2 & NH), 3025 (CH aromatic), 2886 (CH aliphatic), 1682 (C=O); MS: *m*/*z* (intensity%): 260.19 (18) [M$^+$], 241.30 (20), 194.07 (48), 169.59 (62), 138.2 (100), 107.23 (42), 95.01 (44); anal. calcd for $C_{13}H_{16}N_4O_2$ (260.30): C, 59.99; H, 6.20; N, 21.52; found: C, 59.46; H, 6.09; N, 21.80.

*2.1.5.7 6-Amino-5-((butylamino)(phenyl)methyl)pyrimidine-2,4(1H,3H)-dione (**10c**).* White crystal; yield: 43%; m.p. = 304–306 °C; ^{1}H-NMR (DMSO-d_6, 400 MHz): 0.88–0.92 (t, 3H, CH_3), 1.32–1.6 (m, 6H, 3 CH_2), 4.43 (s, 1H, CH), 5.81 (s, 1H, NH), 6.21 (s, 2H, NH_2), 7.1–7.14 (m, 3H, Ar–H), 7.30–7.32 (d, J = 8 Hz, 1H, Ar–H), 7.53–7.55 (d, 1H, Ar–H), 9.64 (brs, 2H, 2 NH); ^{13}C-NMR: 16.19, 27.02, 28.12, 33.34, 49.06, 118.21, 123.4, 132.65, 133.04, 134.8, 150.50, 165.11, 169.73; IR (ν_{max} cm^{-1}): 3229, 3180 (br, NH_2 & NH), 3061 (CH aromatic), 2853, 2850 (CH aliphatic), 1697 (C=O); anal. calcd for $C_{15}H_{20}N_4O_2$ (288.35): C, 62.48; H, 6.99; N, 19.43; found: C, 62.40; H, 6.78; N, 19.75.

*2.1.5.8 6-Amino-5-((dimethylamino)(phenyl)methyl)pyrimidine-2,4(1H,3H)-dione (**10d**).* Red crystal; yield: 96%; m.p. = 255–257 °C; ^{1}H-NMR: 2.54 (s, 6H, 2 CH_3), 4.57 (s, 1H, CH), 6.88 (s, 2H, NH_2), 7.25–7.4 (m, 5H, Ar–H), 10.28 (s, 1H, NH), 10.36 (s, 1H, NH); ^{13}C-NMR: 45.89, 58.56, 83.32, 127.43, 127.53, 128.38, 128.72, 128.91, 139.39, 150.62, 160.57, 166.40; IR (ν_{max} cm^{-1}): 3367, 3181 (NH_2 & NH), 3040 (CH aromatic), 2825 (CH aliphatic), 1682 (C=O); anal. calcd for $C_{13}H_{16}N_4O_2$ (260.13): C, 59.99; H, 6.20; N, 21.52; found: C, 59.42; H, 6.18; N, 21.07.

2.2. Biological activity

2.2.1 *In vitro* cytotoxic activity against the MCF-7 cell line. The cytotoxic activity of the synthesized compounds was assessed against a human tumor cell line representing mammary gland breast cancer (MCF-7). The standard 3-(4,5-dimethyl-2-thiazolyl)-2,5-diphenyl-2*H*-tetrazolium bromide (MTT) method[28–30] was used (Sigma Co., St. Louis, USA), and the cell lines were obtained from American Type Culture Collection

(VA, USA). The quantitative assay relies on the activity of the cells' mitochondria to fragment the tetrazolium ring in MTT. By measuring the produced purplish color spectrophotometrically, it is possible to identify the anticancer activity of various chemicals by observing changes in the number of tumor cells. The anticancer activity is expressed as the concentration of the substance that, when compared with the growth of untreated cells, induces a 50% growth inhibition (IC_{50}, mean ± SD). Cells were grown in the RPMI-1640 medium with 10% fetal bovine serum (Gibco, UK), with 100 U per mL penicillin and 100 g per mL streptomycin added as antibiotics. The cell line was plated in a 96-well plate at a density of 1.0×10^4 cells per well and incubated at 37 °C for 48 h with 5% CO_2. Following incubation, the cells were exposed to various chemical concentrations and incubated for 24 h. Following the drug treatment period, 20 μL of the MTT solution at 5 mg mL^{-1} was added, and the cells were incubated for 4 h. Then, 100 μL of DMSO was added to each well to dissolve the produced purple formazan. Using a plate reader, the colorimetric assay was measured and recorded at 570 nm absorbance (EXL 800, Sigma, MO, USA). Calculated as (the absorbance of the treated sample/the absorbance of the untreated sample) × 100, the relative cell viability was expressed as a percentage.

2.2.2 *In vitro* cytotoxic activity against human normal cells (WI-38). A normal Caucasian fibroblast-like fetal lung cell line (WI-38) was used to evaluate the cytotoxic effect of the highly active substances. Dulbecco's modified Eagle medium (Invitrogen/Life Technologies, MA, USA), 10% fetal bovine serum (GIBCO, UK), 10 g per mL insulin (Sigma, MO, USA), and 1% penicillin/streptomycin were used to culture the cells. The remaining substances and equipment were obtained from either Sigma or Invitrogen. Cells were plated in a 96-well plate for 24 h prior to the MTT assay (cell density: 1.2–1.8 × 10^4 cells per well) in 100 μL of the complete growth media + 100 μL of the examined substance per well.

2.2.3 *In vitro* EGFR-TK enzyme inhibition assay. EGFR and ATP were purchased from Sigma. The EGFR kinase assay kit[31] was used to measure the *in vitro* inhibitory activities of the synthesized compounds against EGFR. First, EGFR and its substrates were incubated with the synthesized compounds in an enzymatic buffer for 5 min. Then, ATP (1.65 μM) was added to the reaction mixture to start the enzymatic reaction. The assay took place for 30 minutes at room temperature. The reaction was stopped by adding detection reagents that contained EDTA. The detection step continued for 1 h, and the IC_{50} values were calculated using GraphPad Prism 5.0. Three independent experiments were carried out for each concentration.

2.3. Molecular docking simulation

Docking was performed based on the methodology outlined in the literature.[32,33] The crystallographic structure of the EGFR kinase domain with gefitinib (PDB ID: 4WKQ)[34] was obtained from the Protein Data Bank (PDB) and prepared for molecular docking by adding hydrogens and minimizing energy using MOE 2024.06. The structure with the lowest energy was selected as the docking receptor. MOE's site finder method was used to identify the active site of EGFR. To validate the docking process, the co-crystallized ligand gefitinib was re-docked onto the active site of EGFR. The root mean square deviation (RMSD) between the re-docked ligand and the co-crystallized position was found to be less than 2 Å. Two-dimensional structures of the synthesized compounds were created using Chem Bio Office and then built from fragment libraries in MOE 2024.06, followed by energy minimization using the MMFF94x force field. Docking was conducted using selected parameters (rescoring functions 1 and 2: London) to investigate and analyze the interactions between the ligands and EGFR active site.

3. Results and discussion

3.1. Chemistry

The reaction of 2-(2-chloropyrimidin-4-yl)isoindoline-1,3-dione 1 (ref. 32 and 33) with sodium sulfide in ethanol afforded the corresponding mercaptan **2**, as shown in Scheme 1. The reaction was assumed to proceed *via* the nucleophilic substitution of halogen by a thiol group. The structure of compound **2** was established as 2-mercaptopyrimidine on the basis of IR, ^{1}H-NMR, ^{13}C-NMR, and mass spectra. The IR spectrum of **2** showed absorption bands at 2413 and 1698 cm^{-1}, assigned to SH and C=O groups, respectively. In addition, the ^{1}H NMR spectrum (DMSO-d_6) of **2** exhibited a singlet signal at δ 12.6 ppm, assigned to SH. The refluxing of **2** with ethyl bromoacetate in absolute ethanol in the presence of potassium carbonate resulted in ((pyrimidine-2-yl)thio)acetate **3** *via* the nucleophilic substitution reaction. The IR spectrum of **3** showed the disappearance of the SH absorption peak along with the appearance of absorption bands at 1749, 2998 and 2850 cm^{-1}, assigned to the carbonyl group of the ester moiety and CH aliphatic, respectively. The chemical structure of **3** was proven by ^{1}H-NMR spectrometry, which revealed a triplet signal at δ 1.03–1.07 ppm, characteristic of the methyl of the ester group; a singlet signal at δ 3.98 ppm, characteristic of S$\underline{CH_2}$ and the presence of a quartet signal at δ 4.15–4.21 ppm, characteristic of the methylene group of the ester moiety. ^{13}C-NMR showed signals for the ester moiety and –SCH_2 at δ 63.04, 14.26, and 45.01 ppm, respectively. Additionally, the hydrazinolysis of **3** afforded 2-((6-(1,3-dioxoisoindolin-2-yl)pyrimidin-2-yl)thio)acetohydrazide **4**, as shown in Scheme 1. The IR spectrum of **4** revealed broad bands at 3332 and 3272 cm^{-1} for NH_2 and NH, respectively. Compound **4** was elucidated by ^{1}H-NMR spectroscopy, which provided exchangeable signals by D_2O at δ 6.76 and 8.89 ppm, characteristic of the NH_2 and NH of the hydrazide moiety, respectively. Acetohydrazide **4** was used as a starting material for the synthesis of different hydrazone derivatives **6a–g** in good to excellent yields through condensation with different aromatic aldehydes **5** (namely, *m*-nitro, *p*-nitro, *p*-chloro, *o*-hydroxy, *p*-hydroxy, *p*-(*N*,*N*-dimethylamino), and 3,4-dimethoxy benzaldehyde) by refluxing with ethanol, as illustrated in Scheme 1. The ^{1}H-NMR and IR spectra of derivatives **6a–g** displayed the disappearance of the –NH_2 band in the –$NHNH_2$ group absorption band moiety. ^{1}H-NMR revealed singlet signals at δ 7.89–9.13 ppm, characteristic of $CH_{hydrazone}$. Additionally, ^{1}H-NMR showed the appearance of –CONHN=

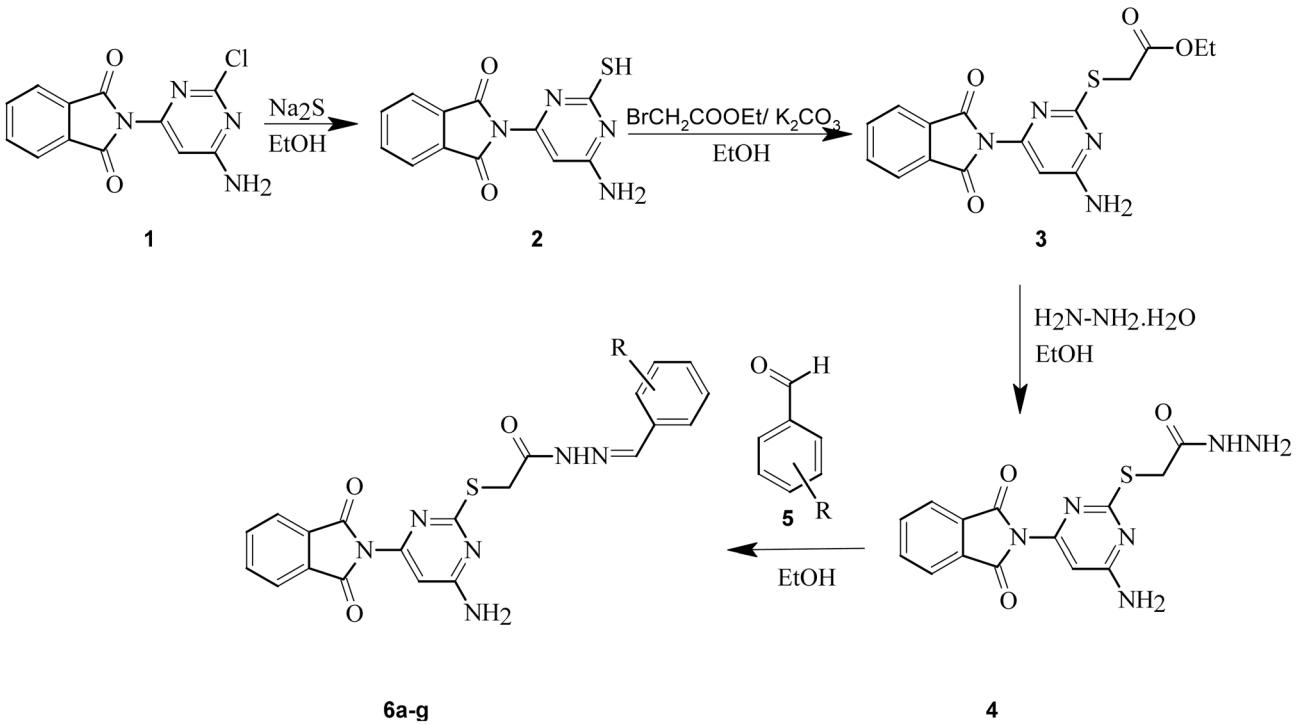

Compd. No.	R	Compd. No.	R
6a	3- NO_2	6e	4- OH
6b	4- NO_2	6f	4- $N(CH_3)_2$
6c	4- Cl	6g	3,4- OCH_3
6d	2- OH		

Scheme 1 Synthesis of the novel hydrazone of 6-(1,3-dioxoisoindolin-2-yl)pyrimidine hybrids (**6a–g**).

CH; for example, compound **6d** showed singlet signals at δ 7.89 and 11.21 ppm, characteristic of $CH_{hydrazone}$ and the OH group (which is exchangeable by D_2O), respectively. The chemical structures of **6a–g** were further confirmed by ^{13}C-NMR, mass spectroscopy and elemental analysis.

Additionally, we synthesized the novel 5-chloro-methylpyrimidine derivatives **8a–c** in good to excellent yields. This was achieved by refluxing 6-aminouracil (**7**)[35–37] with various aromatic aldehydes **5** (namely, benzaldehyde, salicyl-aldehyde, and *p*-dimethylaminobenzaldehyde) in concentrated HCl in a water bath, as shown in Scheme 2. The IR of **8a–c** exhibited absorption peaks at 3040–3070 cm^{-1}, assigned to CH aromatic, with the other expected peaks for the NH_2, NH, and CO groups. In addition, the chemical structure was further confirmed by ^{1}H-NMR, which showed the existence of aromatic protons, D_2O-exchangeable NH_2 and NH (for **8a**), and CH.

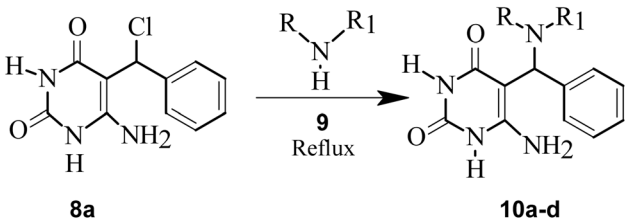

Scheme 3 Synthesis of novel 6-amino-5-((alkylamino)(phenyl) methyl)pyrimidine-2,4(1*H*,3*H*)-dione (**10a–d**).

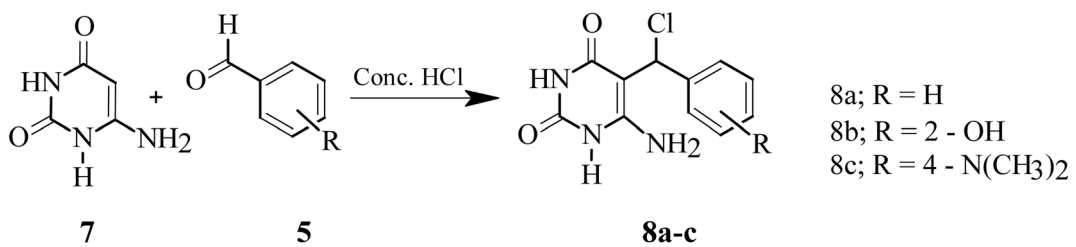

Scheme 2 Synthesis of novel 5-substituted pyrimidine (**8a–c**).

Finally, chloro derivative **8a** underwent a nucleophilic substitution reaction when refluxed with different aliphatic amines **9** (namely, methylamine, ethylamine, butylamine, and dimethylamine) in ethanol in the presence of excess conc. HCl, resulting in the formation of novel 5-(alkylamino(aryl)methyl) uracil derivatives **10a–d**, as shown in Scheme 3. The ^{1}H-NMR spectra of **10a–c** showed singlet signals at δ 5.11–5.81 ppm, assigned to the NH of the alkylamino group, while no signals for this NH were observed for **10d**, with signals at 0.88–2.36 ppm assigned to the CH_3 and CH_2 groups. Additionally, the ^{13}C-NMR spectra of **10a–d** revealed the presence of aliphatic carbons.

Table 1 IC_{50} of **6a–g** and **10a–d** towards MCF-7 and WI38 cell lines compared to thalidomide and gefitinib

	In vitro cytotoxicity IC_{50} (mean ± SD) μM	
	MCF-7	WI38
Thalidomide	13.4 ± 0.5	20.9 ± 1.2
Gefitinib	4.18 ± 0.01	ND
6a	62.0 ± 3.3	42.8 ± 2.3
6b	48.4 ± 2.8	78.2 ± 3.6
6c	31.8 ± 2.0	87.4 ± 4.4
6d	ND	ND
6e	75.4 ± 3.7	33.0 ± 2.1
6f	26.5 ± 1.8	59.6 ± 3.4
6g	19.6 ± 1.5	65.8 ± 3.4
10a	8.6 ± 0.7	46.6 ± 2.5
10b	37.7 ± 2.4	>100
10c	7.6 ± 0.5	54.1 ± 3.1
10d	14.2 ± 1.2	81.4 ± 3.9

3.2. Biological evaluation

3.2.1 ***In vitro*** **cytotoxic activity.** The anti-proliferative effects of **6a–g** and **10a–d** against the human breast cancer cell line (MCF-7) were screened using the standard MTT assay method using thalidomide and gefitinib as reference drugs. According to their anti-proliferative activity, the compounds could be divided into three categories: the compounds with the lowest anti-proliferative activity were **6a** and **6e**; the compounds with moderate activity were **6b**, **6c**, **6f**, **6g** and **10b**; and the compounds that showed high anti-proliferative activity were **10c** and **10d** with IC_{50} of 7.6 ± 0.5 and 8.6 ± 0.7 μM, respectively, compared with those of thalidomide (IC_{50}: 13.4 ± 0.5 μM) and

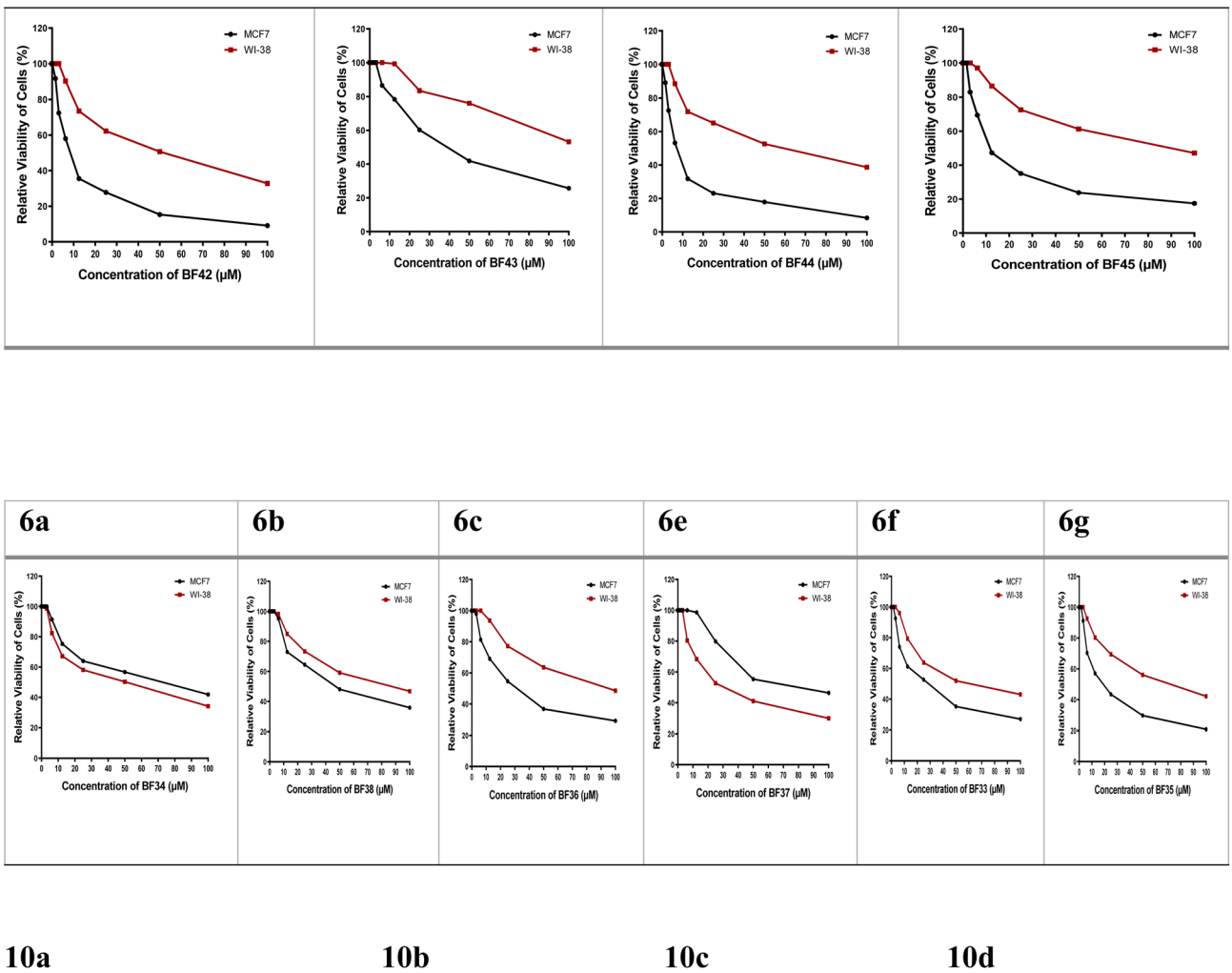

Fig. 3 Viability of MCF-7 and WI38 cell lines at various concentrations of **6a–g** and **10a–d**.

gefitinib (IC_{50}: 4.1 ± 0.01 μM). Structurally, 2-((4-amino-6-(1,3-dioxoisoindolin-2-yl)pyrimidin-2-yl)thio)-*N*′-(alkylbenzylidene) acetohydrazides (**6a–g**) showed moderate to low anti-proliferative activity, while 6-amino-5-((alkylamino)(phenyl) methyl)pyrimidine-2,4(1*H*,3*H*)-diones (**10a–d**) showed the highest anti-tumor activity, and the different alkyl groups showed different activities, where the highest activity was exhibited by **10c** with a butyl amino side chain. Table 1 shows the IC_{50} of compounds **6a–g** and **10a–d** against MCF-7 and WI38 compared to thalidomide and gefitinib.

Compounds **6a–g** and **10a–d** were further investigated for selective cytotoxicity using the fetal lung cell line (WI38) as the normal cell line and thalidomide as the reference drug. Compound **10b** displayed the highest selective cytotoxicity with IC_{50} > 100 μM compared to thalidomide (IC_{50} = 20.9 ± 1.2 μM), as shown in Table 1. Fig. 3 shows the viability of MCF-7 and WI38 cell lines at various concentrations of **6a–g** and **10a–d**.

3.2.2 In vitro EGFR TK enzyme inhibition. In light of their anti-proliferative activity, the most potent compounds, **6c** and **10a–c**, were evaluated for their *in vitro* inhibitory activity against the EGFR TK enzyme using gefitinib as the positive control. Table 2 shows the IC_{50} of **6c** and **10a–c** against the EGFR TK enzyme. **10b** showed the highest inhibitory activity, with an IC_{50} of 0.65 ± 0.02 μM. Table 3 displays the 50% inhibitory concentration (IC_{50}), which is the concentration necessary to inhibit 50% of the EGFR TK enzyme.

3.3. Molecular docking study

The epidermal growth factor receptor tyrosine kinase (EGFR TK) belongs to the receptor tyrosine kinase family, which shares several structural similarities. These include an extracellular binding domain and an intracellular tyrosine kinase domain linked by a transmembrane region and a hydrophobic region. The intracellular domain is composed of an N-lobe and a C-lobe, with the ATP-binding site located between them. The ATP-binding site contains a conserved (Glu) residue essential for catalysis and an activation loop with tyrosine, threonine, or serine residues that undergo phosphorylation to regulate kinase activity. Additionally, all tyrosine kinases have a conserved aspartate-phenyl alanine–glycine (DFG) motif. Most tyrosine kinases also feature a gatekeeper amino acid that controls the access of ligand molecules to the inner hydrophobic pocket where key interactions occur.[33] Gefitinib is a type I EGFR TK inhibitor that specifically binds to the active form of EGFR TK, where the Asp residue of the DFG motif adopts an "in-plane conformation", positioning the Asp residue towards the ATP-binding site and the ligand. Gefitinib forms a H-bond interaction with Asp800 and additional H-bonds with Leu718, Leu788, Cys775, and the critical amino acid Met793 at the N1 of its quinazoline core, which functions as a H-bond acceptor group. Furthermore, gefitinib forms a network of hydrogen bonds mediated by water molecules (w1 and w2) with amino acids Gln791, Thr854, and Thr790.[4] Fig. 4 shows gefitinib at the ATP binding site of EGFR-TK (PDB ID: 4WKQ). When docked into the ATP binding site of EGFR-TK, **6c** showed a binding mode similar to that of gefitinib, forming a H-bond interaction with the key amino acid Met793 at the carbonyl group of the aceto-hydrazide linker as a hydrogen bond acceptor, while the amino group at the pyrimidine acted as a hydrogen bond donor, forming an additional H-bond interaction with Arg541. It also formed a number of hydrophobic interactions with key amino acids including Leu544, Lys728, Leu715, Val725 and Pro794, as shown in Fig. 5. **10b** was also capable of forming H-bond interactions with the key amino acid Met793, and it formed a π–H interaction with Lys745 and a number of hydrophobic interactions with Leu844, Lys745, Val726 and Thr790, as shown in Fig. 6. There was an agreement in the molecular docking and *in vitro* enzyme inhibition results, which could be used to explain the anti-proliferative activity of the synthesized compounds.

Table 2 The *in vitro* inhibitory activity of compounds **6a–c**, **6e–g** and **10a–d** against the WI-38 cell line compared with thalidomide

Cpd no.	Cytotoxicity IC_{50} (mean ± SD), μM
Thalidomide	20.85 ± 1.2
6a	42.75 ± 2.3
6b	78.29 ± 3.6
6c	87.41 ± 4.4
6e	33.03 ± 2.1
6f	59.61 ± 3.4
6g	65.76 ± 3.4
10a	46.59 ± 2.5
10b	>100
10c	54.05 ± 3.1
10d	81.36 ± 3.9

Table 3 IC_{50} of **6c**, **10a–c**, and gefitinib against the EGFR TK enzyme

Compound	EGFR IC_{50} (mean ± SD) μM
6c	0.88 ± 0.03
10a	4.60 ± 0.11
10b	0.65 ± 0.02
10c	0.99 ± 0.03
Gefitinib	0.033 ± 0.011

3.4. *In silico* pharmacokinetic profile

Drug-likeness is defined by molecular, structural, and physicochemical properties, as outlined in Lipinski's Rule of Five, which includes molecular weight, hydrogen bond donors, hydrogen bond acceptors, and partition coefficient (log *P*).[38] In this study, the drug-likeness and ADME properties of synthesized compounds **6c** and **10b** were evaluated using Admetlab 2.0 (ref. 39) with gefitinib as a reference. Both compounds complied with Lipinski's rule without any violations. Their molecular weights were 466 g mol^{-1} (**6c**) and 260 g mol^{-1} (**10b**), satisfying the rule of molecular weight ≤ 500 g mol^{-1}. The partition coefficients (log *P*) of 4.09 (**6c**) and 0.57 (**10b**) were within the acceptable range (log *P* ≤ 5). Additionally, the topological polar surface areas (TPSAs), crucial for assessing the polar atom–surface interaction, were 130 Å (**6c**) and 103 Å (**10b**), well below

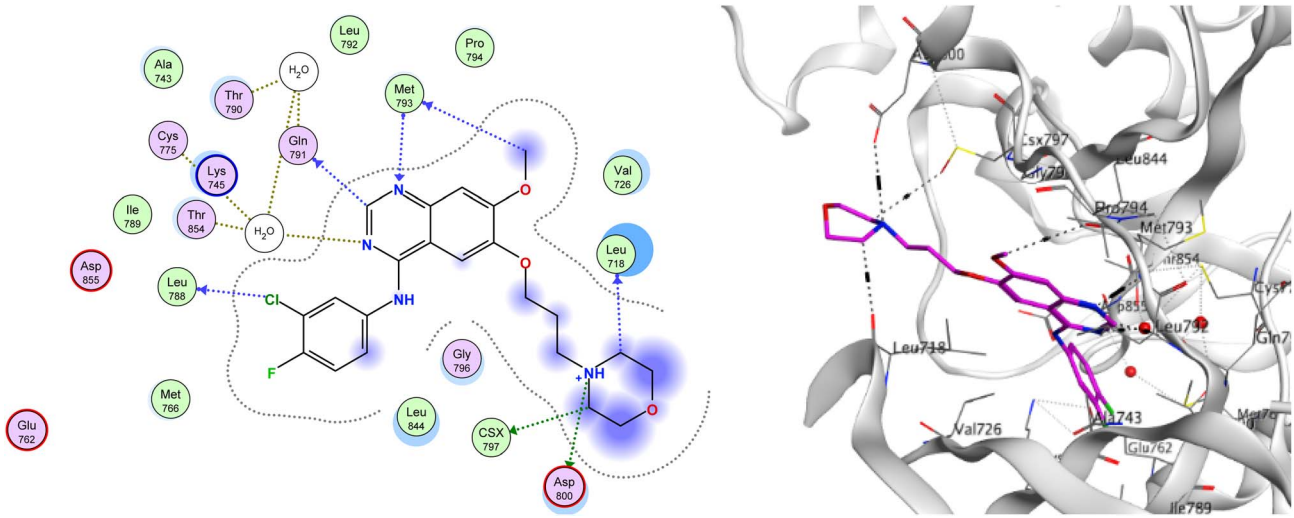

Fig. 4 2D and 3D representations of gefitinib at the EGFR (PDB ID: 4WKQ) ATP binding site.

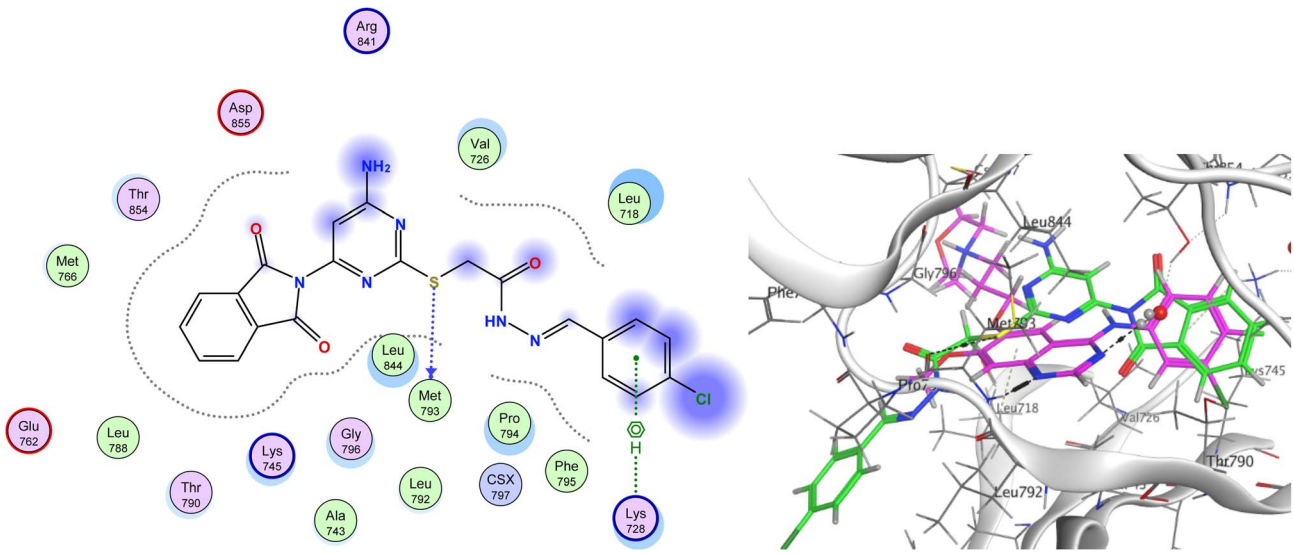

Fig. 5 2D and 3D representation of **6c** and the alignment of **6c** (Green) with gefitinib (purple) at the EGFR (PDB ID: 4WKQ) ATP binding site.

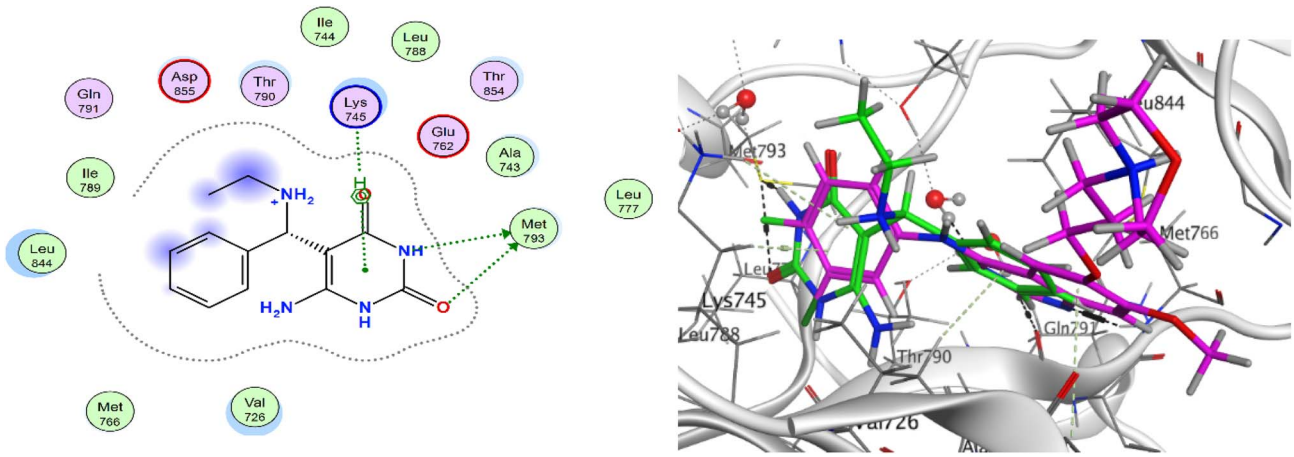

Fig. 6 2D and 3D representations of **10b** and the alignment of **10b** (green) with gefitinib (purple) at the EGFR (PDB ID: 4WKQ) ATP binding site.

the threshold of ≤160 Å.[40] Unlike gefitinib (TPSA = 68 Å), which violated Pfizer's rule by having too low a TPSA, both compounds fell within the ideal range. Both compounds displayed flexibility with an acceptable number of rotatable bonds. They also adhered to Lipinski's thresholds for hydrogen bond acceptors (≤12) and donors (≤7). The detailed physicochemical properties and drug-likeness data are provided in SI. ADME analysis revealed that compound **6c** was moderately soluble ($\log S = -5.66$), while **10b** was soluble ($\log S = -2.61$), with solubility categorized as insoluble < −10 < poorly soluble < −6 < moderately soluble < −4 < soluble < −2 < very soluble < 0 < highly soluble.[41] Compound **10b** showed high gastrointestinal absorption, suggesting its efficient entry into the bloodstream, whereas **6c** lacked gastrointestinal absorption.[42] Neither compound penetrated the blood–brain barrier, indicating no potential CNS side effects, similar to gefitinib. Both **6c** and **10b** showed no liver toxicity risks and were identified as non-substrates and non-inhibitors of cytochrome P450 2D6, unlike gefitinib, which displayed potential liver toxicity and acted as both a substrate and an inhibitor of this enzyme. Toxicity evaluations showed that **6c** and **10b** were non-carcinogenic and non-toxic in the Ames test and passed acute oral toxicity tests. In contrast, gefitinib exhibited both carcinogenic tendencies and acute oral toxicity in rat models. These findings highlight the superior safety profile of compounds **6c** and **10b** compared to gefitinib.

4. Conclusion

In conclusion, 6-(1,3-dioxoisoindolin-2-yl)pyrimidine (**6a–g**), 6-amino-5-(chloro(aryl)-methyl) pyrimidine-2,4(1*H*,3*H*)-dione (**8a–e**) and 6-amino-5-((alkylamino)(phenyl)methyl) pyrimidine-2,4(1*H*,3*H*)-dione (**10a–d**) were synthesized as aminopyrimidine hybrids. *In silico* ADMET studies showed that compounds are good oral bioavailable drug candidates that can pass the gut wall but not the blood–brain barrier, with no potential side effects to the liver. Compounds showed no toxicity using the *in silico* toxicity prediction tool. The compounds demonstrated good oral bioavailability and good gastrointestinal absorption with no possible adverse effects on the liver or CNS. In addition, the compounds showed selective cytotoxicity against mammary gland breast cancer (MCF-7) compared to thalidomide as a reference drug. Compound **10b** displayed high activity against the MCF-7 cell line. **6c** and **10b** showed *in vitro* inhibitory activity toward the EGFR-TK enzyme and were capable of binding at the EGFR-TK binding site in an inhibitory mode.

Conflicts of interest

The authors have no competing interests to declare.

Data availability

Supplementary information: all data including experimental procedures, compound characterization and NMR spectra are recorded in the SI. See DOI: **https://doi.org/10.1039/d5ra02524a**.

Acknowledgements

This research did not receive any specific grant from funding agencies in the public, commercial, or not-for-profit sectors. We gratefully acknowledge CCMML (Computational Chemistry and Molecular Modelling Lab), Pharmaceutical Organic Chemistry Department, Faculty of Pharmacy, Mansoura University, where the molecular docking simulations were carried out.

References

1 Z. Dembic, Antitumor drugs and their targets, *Molecules*, 2020, **25**(23), 5776.
2 N. Karachaliou, *et al.*, EGFR first-and second-generation TKIs—there is still place for them in EGFR-mutant NSCLC patients, *Transl. Cancer Res.*, 2019, **8**(Suppl 1), S23.
3 B. Sharma, V. J. Singh and P. A. Chawla, Epidermal growth factor receptor inhibitors as potential anticancer agents: An update of recent progress, *Bioorg. Chem.*, 2021, **116**, 105393.
4 T. Amelia, *et al.*, Structural insight and development of EGFR tyrosine kinase inhibitors, *Molecules*, 2022, **27**(3), 819.
5 H. Masuda, *et al.*, Role of epidermal growth factor receptor in breast cancer, *Breast Cancer Res. Treat.*, 2012, **136**, 331–345.
6 F. D. M. Opo, *et al.*, Pharmacophore-based virtual screening approaches to identify novel molecular candidates against EGFR through comprehensive computational approaches and in-vitro studies, *Front. Pharmacol*, 2022, **13**, 1027890.
7 M. J. Akhtar, *et al.*, Synthesis of stable benzimidazole derivatives bearing pyrazole as anticancer and EGFR receptor inhibitors, *Bioorg. Chem.*, 2018, **78**, 158–169.
8 B. Sever, *et al.*, Design, synthesis and biological evaluation of a new series of thiazolyl-pyrazolines as dual EGFR and HER2 inhibitors, *Eur. J. Med. Chem.*, 2019, **182**, 111648.
9 M. A. Elbastawesy, *et al.*, Novel Pyrazoloquinolin-2-ones: Design, synthesis, docking studies, and biological evaluation as antiproliferative EGFR-TK inhibitors, *Bioorg. Chem.*, 2019, **90**, 103045.
10 H.-A. S. Abbas and S. S. Abd El-Karim, Design, synthesis and anticervical cancer activity of new benzofuran–pyrazol-hydrazono-thiazolidin-4-one hybrids as potential EGFR inhibitors and apoptosis inducing agents, *Bioorg. Chem.*, 2019, **89**, 103035.
11 M. S. Alsaid, *et al.*, Discovery of Benzo [g] quinazolin benzenesulfonamide derivatives as dual EGFR/HER2 inhibitors, *Eur. J. Med. Chem.*, 2017, **141**, 84–91.
12 M. M. Ghorab, *et al.*, Benzo [g] quinazolin-based scaffold derivatives as dual EGFR/HER2 inhibitors, *J. Enzyme Inhib. Med. Chem.*, 2018, **33**(1), 67–73.
13 M. M. Ghorab, M. S. Alsaid and A. M. Soliman, Dual EGFR/HER2 inhibitors and apoptosis inducers: New benzo [g] quinazoline derivatives bearing benzenesulfonamide as anticancer and radiosensitizers, *Bioorg. Chem.*, 2018, **80**, 611–620.
14 K. V. Sairam, *et al.*, Cytotoxicity studies of coumarin analogs: design, synthesis and biological activity, *RSC Adv.*, 2016, **6**(101), 98816–98828.

15 S. Dhawan, *et al.*, Synthesis, computational studies and antiproliferative activities of coumarin-tagged 1, 3, 4-oxadiazole conjugates against MDA-MB-231 and MCF-7 human breast cancer cells, *Bioorg. Med. Chem.*, 2018, **26**(21), 5612–5623.

16 S. K. J. Shaikh, *et al.*, Microwave-Expedited Green Synthesis, Photophysical, Computational Studies of Coumarin-3-yl-thiazol-3-yl-1, 2, 4-triazolin-3-ones and Their Anticancer Activity, *ChemistrySelect*, 2018, **3**(16), 4448–4462.

17 M. T. Gabr, *et al.*, Synthesis, *in vitro* antitumor activity and molecular modeling studies of a new series of benzothiazole Schiff bases, *Chin. Chem. Lett.*, 2016, **27**(3), 380–386.

18 L. Zhang, *et al.*, Design, synthesis and cytotoxic evaluation of a novel series of benzo [d] thiazole-2-carboxamide derivatives as potential EGFR inhibitors, *Med. Chem. Res.*, 2017, **26**, 2180–2189.

19 H. A. El-Sherief, *et al.*, Synthesis, anticancer activity and molecular modeling studies of 1, 2, 4-triazole derivatives as EGFR inhibitors, *Eur. J. Med. Chem.*, 2018, **156**, 774–789.

20 A. M. Srour, *et al.*, Design, synthesis, biological evaluation, QSAR analysis and molecular modelling of new thiazol-benzimidazoles as EGFR inhibitors, *Bioorg. Med. Chem.*, 2020, **28**(18), 115657.

21 X.-X. Tao, *et al.*, Design, synthesis and biological evaluation of pyrazolyl-nitroimidazole derivatives as potential EGFR/HER-2 kinase inhibitors, *Bioorg. Med. Chem. Lett.*, 2016, **26**(2), 677–683.

22 A. A. Gaber, *et al.*, Design, synthesis and anticancer evaluation of 1H-pyrazolo [3, 4-d] pyrimidine derivatives as potent EGFRWT and EGFRT790M inhibitors and apoptosis inducers, *Bioorg. Chem.*, 2018, **80**, 375–395.

23 D. Zhang, *et al.*, Synthesis and antitumor evaluation of novel 4-anilino-7, 8-dihydropyrido [4, 3-d] pyrimidine-6 (5H)-carboxylate derivatives as potential EGFR inhibitors, *Arch. Pharm.*, 2018, **351**(9), 1800110.

24 Y. Hao, *et al.*, Design, Synthesis, and biological evaluation of pyrimido [4, 5-d] pyrimidine-2, 4 (1 h, 3 h)-diones as potent and selective epidermal growth factor receptor (EGFR) inhibitors against L858R/T790M resistance mutation, *J. Med. Chem.*, 2018, **61**(13), 5609–5622.

25 S. A. Elmetwally, *et al.*, Design, synthesis and anticancer evaluation of thieno [2, 3-d] pyrimidine derivatives as dual EGFR/HER2 inhibitors and apoptosis inducers, *Bioorg. Chem.*, 2019, **88**, 102944.

26 Z. Xie, *et al.*, Discovery of 4, 6-pyrimidinediamine derivatives as novel dual EGFR/FGFR inhibitors aimed EGFR/FGFR1-positive NSCLC, *Eur. J. Med. Chem.*, 2020, **187**, 111943.

27 A. Barbarossa, *et al.*, Recent advances in the development of thalidomide-related compounds as anticancer drugs, *Curr. Med. Chem.*, 2022, **29**(1), 19–40.

28 I. H. Eissa, A. M. El-Naggar and M. A. El-Hashash, Design, synthesis, molecular modeling and biological evaluation of novel 1H-pyrazolo [3, 4-b] pyridine derivatives as potential anticancer agents, *Bioorg. Chem.*, 2016, **67**, 43–56.

29 T. Mosmann, Rapid colorimetric assay for cellular growth and survival: application to proliferation and cytotoxicity assays, *J. Immunol. Methods*, 1983, **65**(1–2), 55–63.

30 G. Ciapetti, *et al.*, In vitro evaluation of cell/biomaterial interaction by MTT assay, *Biomaterials*, 1993, **14**(5), 359–364.

31 J. L. Nakamura, The epidermal growth factor receptor in malignant gliomas: pathogenesis and therapeutic implications, *Expert Opin. Ther. Targets*, 2007, **11**(4), 463–472.

32 W. Shehta, *et al.*, Synthesis and *in vitro* study of pyrimidine–phthalimide hybrids as VEGFR2 inhibitors with antiproliferative activity, *Future Med. Chem.*, 2023, **15**(8), 661–677.

33 J. H. Park, *et al.*, Erlotinib binds both inactive and active conformations of the EGFR tyrosine kinase domain, *Biochem. J.*, 2012, **448**(Pt 3), 417.

34 W. Shehta, *et al.*, Synthesis, *In Vitro* and *In Silico* Molecular Docking Studies of Novel Phthalimide–Pyrimidine Hybrid Analogues to Thalidomide as Potent Antitubercular Agents, *SynOpen*, 2025, **9**, 73–83.

35 S. S. Chavan, R. U. Shelke and M. S. Degani, Carboxylic acid-catalyzed one-pot synthesis of cyanoacetylureas and their cyclization to 6-aminouracils in guanidine ionic liquid, *Monatsh. Chem.*, 2013, **144**, 399–403.

36 S. Youssif, S. El-Bahaie and E. Nabih, Synthesis and antimicrobial activities of pyrido[2,3-d] pyrimidine, pyridotriazolopyrimidine, triazolopyrimidine, and pyrido [2,3-d:6,5d'] dipyrimidine derivatives, *J. Chem. Res.*, 1999, **23**, 112.

37 S. Youssif and S. F. Mohamed, 6-Amino-2-thio- and 6-Aminouracils as Precursors for the Synthesis of Antiviral and Antimicrobial Methylenebis(2-thiouracils), Tricyclic Pyrimidines, and 6-Alkylthiopurine-2-ones, *Monatsh. Chem.*, 2008, **139**, 161.

38 B. Farag, F. Agili, S. El-Kalyoubi, S. A. Said, S. Youssif and W. S. Shehta, Molecular Docking and Anticancer Activity of Some 5-Aryl-5,10-dihydropyrido[2,3-d:6,5-d′]dipyrimidine-2,4,6,8-tetraone Derivatives and Pyrido[2,3-d]pyrimidines, *ChemistrySelect*, 2022, **7**, e202103834.

39 G. Xiong, *et al.*, ADMETlab 2.0: an integrated online platform for accurate and comprehensive predictions of ADMET properties, *Nucleic Acids Res.*, 2021, **49**(W1), W5–W14.

40 A. Daina, O. Michielin and V. Zoete, iLOGP: a simple, robust, and efficient description of n-octanol/water partition coefficient for drug design using the GB/SA approach, *J. Chem. Inf. Model.*, 2014, **54**(12), 3284–3301.

41 J. Ali, *et al.*, In silico prediction of aqueous solubility using simple QSPR models: the importance of phenol and phenol-like moieties, *J. Chem. Inf. Model.*, 2012, **52**(11), 2950–2957.

42 A. Daina and V. Zoete, A boiled-egg to predict gastrointestinal absorption and brain penetration of small molecules, *ChemMedChem*, 2016, **11**(11), 1117–1121.